Separation Science and Technology
Publication details, including instructions for authors and subscription information:
http://www.informaworld.com/smpp/title~content=t713708471

Adsorption of As(III), As(V), Cd(II), Cu(II), and Pb(II) from Aqueous Solutions by Natural Muscovite

Jung-Seok Yang[a]; Ju Young Lee[a]; Young-Tae Park[a]; Kitae Baek[b]; Jaeyoung Choi[a]
[a] Korea Institute of Science and Technology (KIST)-Gangneung Institute, Gangneung, Republic of Korea [b] Department of Environmental Engineering, Kumoh National Institute of Technology (KIT), Gumi, Republic of Korea

Online publication date: 22 March 2010

To cite this Article Yang, Jung-Seok , Lee, Ju Young , Park, Young-Tae , Baek, Kitae and Choi, Jaeyoung(2010) 'Adsorption of As(III), As(V), Cd(II), Cu(II), and Pb(II) from Aqueous Solutions by Natural Muscovite', Separation Science and Technology, 45: 6, 814 — 823
To link to this Article: DOI: 10.1080/01496391003609023
URL: http://dx.doi.org/10.1080/01496391003609023

Separation Science and Technology, 45: 814–823, 2010

ISSN: 0149-6395 print/1520-5754 online
DOI: 10.1080/01496391003609023

Taylor & Francis
Taylor & Francis Group

Adsorption of As(III), As(V), Cd(II), Cu(II), and Pb(II) from Aqueous Solutions by Natural Muscovite

Jung-Seok Yang,[1] Ju Young Lee,[1] Young-Tae Park,[1] Kitae Baek,[2] and Jaeyoung Choi[1]

[1]*Korea Institute of Science and Technology (KIST)-Gangneung Institute, Gangneung, Republic of Korea*
[2]*Department of Environmental Engineering, Kumoh National Institute of Technology (KIT), Gumi, Republic of Korea*

Various parameters were tested for the application of natural muscovite (NM) in the removal of metals from aqueous solutions: contact time, pH, ionic strength, and initial metal concentrations. Kinetic studies showed that the pseudo-second-order model explains well the sorption process. The adsorption of metals was greatly influenced by solution pH but not by ionic strength. The results from isotherm studies agreed more with the Freundlich isotherm model than with the Langmuir isotherm model. The adsorbed quantity of metals by NM was lower than that by the purified mica. These results suggested that the composition and surface characteristics of natural minerals may seriously influence applications for water purification.

Keywords adsorbent; arsenic; complexes; metals; mica

INTRODUCTION

Water pollution by metals is a serious problem because of their toxicity and resistance to biodegradation. To remove metals from aqueous streams, various technologies have been developed such as electrochemical treatment, chemical and physical treatment, biological treatment, membrane processes, and adsorption (1–9). Among these technologies, adsorption is the most convenient and popular method for the removal of metals from aqueous systems.

Muscovite micas are phyllosilicate minerals consisting of silica layers sandwiched between octahedral aluminum layers and have highly perfect basal cleavage (10–12). The permanent lattice charge of muscovite is generated by the substitution of Si with Al and the lattice charge locates close to the cleaved surface plane. It is expected to enhance the formation of inner-sphere complexation (13). The negative structural charge of the each muscovite layer is balanced by surface and interlayer K^+ (14). Because basal surfaces of muscovite mica are readily produced by mechanical cleavage, the interaction between mica and inorganic cation has been extensively studied (13, 15–17). In addition, a number of sorption studies have been performed for metals by using mica. Chakraborty et al. (10) observed that arsenic sorption onto muscovite and biotite increases with pH, maximizes at a pH of 4.2–5.5, and decreases at higher pH. Charlet et al. (18) reported that arsenate may be reduced on the surface of muscovite through their study of proton-induced X-ray emission (PIXE) and X-ray photoelectron spectroscopy (XPS). Tiwari et al. (19) studied the application of natural sericite for the removal of Cu(II) and Pb(II) from aqueous solutions. Although muscovite has been studied as a model mica, studies using natural muscovite (NM) are very few.

In this study, the adsorption of metals with NM was investigated by batch tests. Initially, the specifications for NM related to the removal of metals were investigated. The adsorption kinetics and isotherm were then tested. To elucidate the adsorption mechanism, the effects of pH and ionic strength were also tested.

MATERIALS AND METHODS

Characterization of NM

NM was obtained from Samkyung Mining Co., Ltd. (Gangneung, Gangwon-do, Korea). The chemical composition of NM was determined by automatic sequential X-ray fluorescence (XRF, Rigaku ZSX 100e, Japan) and is given in Table 1. The particle size distribution was analyzed by particle size analyzer (LS230, Beckman Coulter, USA). The mean particle diameter of NM was 7.5 μm. The silt fraction was 85% with the sand and clay fractions being 1.6% and 13.4%, respectively (Table 2). The BET surface area of NM was determined by N_2 adsorption (Tristar 3000, Micromeritics Instrument Co., USA) and was

Received 24 May 2009; accepted 4 January 2010.
Address correspondence to Jaeyoung Choi, Korea Institute of Science and Technology (KIST)-Gangneung Institute, Gangneung 210-703, South Korea. Tel.: +82-33-650-7301; Fax: +82-33-650-7199. E-mail: jchoi@kist.re.kr

TABLE 1
Composition of metal oxides in NM

Component	Mass %
SiO_2	61.32
Al_2O_3	23.90
K_2O	7.12
CaO	2.48
MgO	2.07
Fe_2O_3	1.31
TiO_2	0.26
Na_2O	0.15
Other	0.15
LOI[a]	1.27

[a]Loss on ignition.

$1.27\,m^2\,g^{-1}$. The surface of NM was analyzed by field emission scanning electron microscope (FE-SEM, Hitachi Su-70, Japan). NM is composed of various sheets, which is shown in the FE-SEM image (Fig. 1(a)). The mineral composition of NM was identified through X-ray diffraction (XRD, X'Pert Pro XRD, PANalytical, Netherlands). The XRD patterns strongly suggest that the NM consisted of 88% muscovite and 12% quartz (Fig. 1(b)). The cation exchange capacity (CEC) was measured by the sodium acetate method and was found to be 0.28 cmol kg^{-1}. The NM was dried at 105°C for 24 h and sieved to a size below 75 μm (200 mesh) for the experiments.

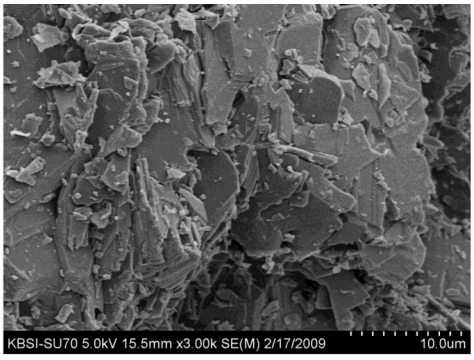

(a)

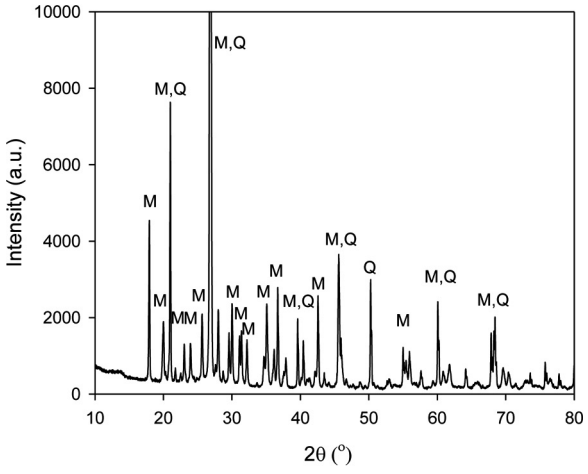

(b)

FIG. 1. (a) FE-SEM image and (b) XRD pattern of NM (M: muscovite, Q: quartz).

Reagents

Stock solutions (100 and 1000 mg/L) of As(III) and As(V) were prepared with $NaAsO_2$ (Sigma, USA) and $Na_2HAsO_4 \cdot 7H_2O$ (Fluka, USA), respectively. Stock solutions (100 and 1000 mg/L) of the metals Cd, Cu, and Pb were prepared with their nitrate salts $Cd(NO_3)_2 \cdot 4H_2O$, $Cu(NO_3)_2 \cdot 3H_2O$, and $Pb(NO_3)_2$ (Sigma-Aldrich, USA), respectively. Sodium nitrate and sodium hydroxide were purchased from Junsei Chemical Co. (Japan). Nitric acid was purchased from Samchun Pure Chemical Co., Ltd. (Korea). De-ionized water was prepared using the Millipore water purification system (Millipore, USA).

Batch Experiments

All adsorption experiments were conducted at 20°C. To evaluate metals removal by adsorption process without precipitation, all experiments were conducted at pH 6. As the results of MINTEQA2, which is an equilibrium speciation model and was released by the USEPA, simulation for the speciation of As(III), As(V), Cd(II), Cu(II), and Pb(II), the precipitation does not occur at pH. All the experiments were performed under open atmospheric conditions.

TABLE 2
BET surface area and particle size distribution of NM

Surface area ($m^2\,g^{-1}$)	Sand (>50 μm, %)	Silt (2–50 μm, %)	Clay (<2 μm, %)
1.27	1.6	85.0	13.4

The dissolution of K, Al, Ca, Mg, Fe, and Si from NM was conducted with 1 g of NM and 25 ml of a solution containing 0–1.5 mL of 1 M HNO_3 in a 50-mL conical tube. Samples were placed on a reciprocating shaker table and agitated for 24 h and then the samples were filtered through a 0.45-μm membrane filter. The concentration of metals in the filtrate was analyzed with an inductively coupled plasma optical emission spectrometer (ICP-OES, Varian 730-ES, USA). The final pH of the solution was measured with a pH meter (Mettler Toledo 8603, USA). The dissolution kinetic experiment was carried out with 20 g of NM and 500 mL of a solution containing 14 mL of 1 M HNO_3 in a 1 L beaker. The solution was mixed with an overhead stirrer. 5 mL of aquatic solution was taken at 0, 1, 5, 10, 20, 30, 60, 90, 120, 240, and 360 min and the pH and element

concentrations of the solutions were measured after filtration.

Adsorption isotherms were conducted with 1 g of NM and 25 mL of a solution containing 2.5 mL of 0.1 M $NaNO_3$ solution for background ionic strength. Metal stock solutions were added to produce the final concentration range from 0 to 100 mg L^{-1}, and a small amount of 1 M HNO_3 was added to adjust the final pH to 6. The samples were equilibrated with air for 24 h at 100 rpm in an orbital shaker and then filtered through a 0.45-μm membrane filter. The final pH and metal concentrations were measured by a pH meter and ICP-OES, respectively. The effects of ionic strength were investigated by varying the $NaNO_3$ concentration from 0 to 0.5 with the procedure used for adsorption isotherm experiments: 10 mg L^{-1} of the total metal concentration with a final pH of 6.0 and ionic strength of 0.01 M $NaNO_3$.

Adsorption pH edge studies were carried out by mixing 10 mg L^{-1} of each metal (As, Cd, Cu, and Pb) with 1 g of NM in a 0.01 M $NaNO_3$ solution. 0–1.5 mL of 1 M HNO_3 was added to adjust the final pH to within 2–10. The samples were equilibrated for 24 h at 100 rpm on an orbital shaker and then filtered through a 0.45-μm membrane filter.

The adsorption kinetic experiments were carried out with 1 g of NM and 25 mL of a solution containing 0.7 mL of 1 M HNO_3, 0.01 M of $NaNO_3$, and 10 mg L^{-1} of each metal (As, Cd, Cu, and Pb) in a 50-mL conical tube. The samples were shaken for 1, 5, 10, 15, 20, 30, 60, 90, 120, and 240 min. After the time, the pH and element concentrations of the solutions were measured after filtration.

The adsorption percentages were calculated from the difference between the initial and the final metal concentrations.

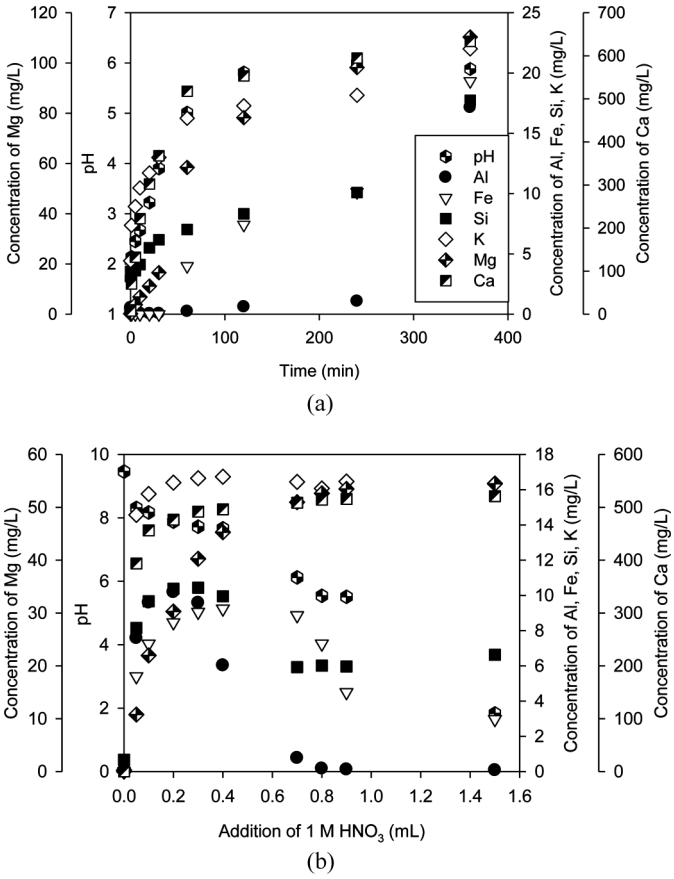

FIG. 2. (a) Dissolution rate of 1 g of NM in 25 mL of a solution containing 0.7 mL of 1 M HNO_3 and (b) dissolved element concentrations and pH of 25 mL solutions containing 1 g of NM and 0–1.5 mL of 1 M HNO_3.

RESULTS AND DISCUSSION

Dissolution of NM

Figure 2 shows the dissolution kinetics of NM and concentrations of the dissolved elements in NM after the addition of HNO_3. In the dissolution kinetics for NM, the initial pH was lower than 2 and reached 6 after a gradual increase. The major dissolved element in NM was calcium which showed an increase in concentration with decreasing pH. Small amounts of K, Al, Mg, Fe, and Si were also dissolved. During the dissolution of the dissolved elements, hydroxyl ions may be released or hydrogen ions consumed, both of which increase the pH. The dissolute concentration of Al, Fe, and Si was maximized at pH 7.5. There was no great change of K and Mg concentrations in the pH 2–8. Because the K concentration was similar with pH range from 2 to 8, the dissolute K^+ is expected as surface K^+ which was desorbed when the amount of available H_3O^+ substantially exceeds the amount of K^+ on the muscovite surface (15). According to the XRD results, the major minerals of NM were muscovite and quartz, and their composition elements are K, Al, and Si. This means that the dissolution of impurities in NM highly affected the pH of solutions. Because the adsorption of metals is affected by solution pH and the dissolved elements compete with metals for adsorption onto NM, the quantity and composition of impurities in NM can be important factors. It is possible that the adsorption of metals onto muscovite could be minimized by the adsorption of released elements (Si, Al, Ca, Mg, and Fe) from muscovite. According to Park et al. (15), the effective surface charge density of the muscovite irreversibly reduced after interaction with the low pH solution. Additionally the zero point charge (ZPC) of minerals affects the adsorption of metals. In Fig. 2(b), the pH of the solution containing NM converged at two points (pH 5.4 and 2) as HNO_3 was added. These may have been caused by the ZPCs of muscovite and silica. The ZPC of muscovite is 5.25 (10), while that of silica is approximately 2–3 (19).

Adsorption Kinetics

To investigate the adsorption mechanism, three types of adsorption kinetic model—pseudo-first-order (20–22), pseudo-second-order (21–24), and Weber and Morris (25)—were employed.

The pseudo-first-order rate equation is given as (20–22):

$$\ln(q_e - q_t) = \ln q_e - k_1 t$$

where q_t and q_e (mg g^{-1}) are the amounts of metal ions adsorbed at equilibrium and t (min), respectively, and k_1 is the rate constant of the equation (min^{-1}).

The pseudo-second-order kinetic model has the following form (21–24):

$$\frac{t}{q_t} = \frac{1}{k_2 q_e^2} + \frac{t}{q_e}$$

where k_2 (g mg^{-1} min^{-1}) is a rate constant for the second-order equation. The pseudo second-order kinetic model reflects rate-limiting steps, which may consist of chemisorptions and the diffusion process.

To elucidate its mechanism, an intraparticle diffusion model using the Weber and Morris equation (25) was applied. The model is expressed as follows (25–26):

$$q_t = k_{ip} t^{1/2}$$

where k_{ip} is the intraparticle diffusion rate constant. According to this model, if adsorption of a solute is controlled by the intraparticle diffusion process, the plot of q_t versus $t^{1/2}$ gives a straight line.

The kinetic experiment data and constants of the above equations are summarized in Fig. 3 and Table 3, respectively. In the results, the pseudo-second-order model was well fitted with the experimental data with good correlation coefficients ($r^2 = 0.945$–1.000), while the pseudo-first-order kinetic model ($r^2 = 0.117$–0.979) and the Weber and Morris equation ($r^2 = 0.212$–0.964) did not match with the experimental data. The calculated sorption capacity $q_{m(cal)}$ was

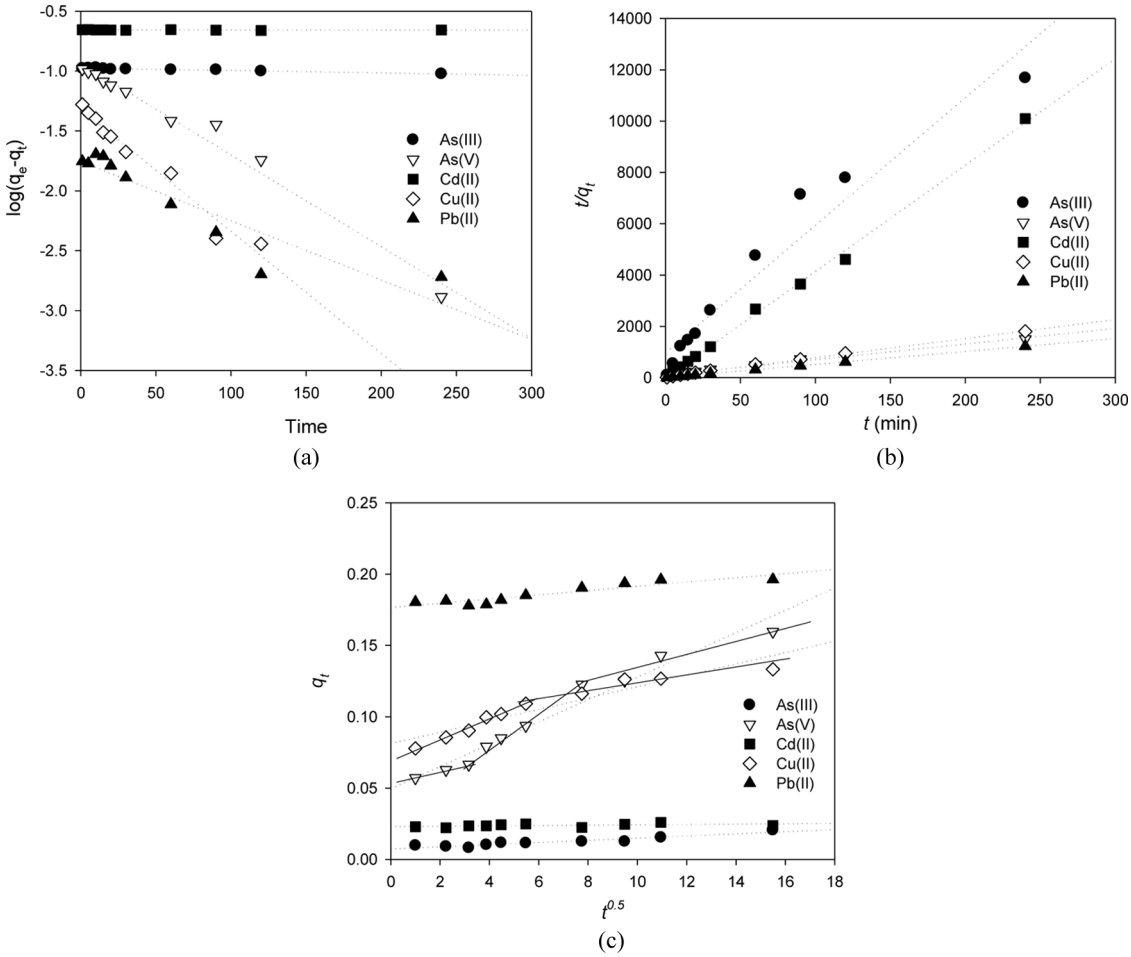

FIG. 3. (a) Pseudo-first-order, (b) pseudo-second-order, and (c) Weber and Morris model fitting for removal kinetics of metals by NM.

TABLE 3
Summary of adsorption kinetic parameters for the pseudo-first-order, pseudo-second-order, and Weber and Morris model

		Pseudo-first-order			Pseudo-second-order			Weber and Morris	
	$q_{e\ (exp)}$ (mg g^{-1})	$q_{e\ (cal)}$ (mg g^{-1})	k_1 (min^{-1})	r^2	$q_{e\ (cal)}$ (mg g^{-1})	k_2 (gmg^{-1} min^{-1})	r^2	k_{ip} (min$^{-0.5}$)	r^2
As(III)	0.115	0.106	4.62E-04	0.945	0.020	5.36E-05	0.945	7.54E-04	0.892
As(V)	0.161	0.116	1.76E-02	0.979	0.165	6.65E-04	0.989	7.82E-03	0.964
Cd(II)	0.025	0.220	2.44E-05	0.117	0.025	1.23E-02	0.998	1.20E-04	0.212
Cu(II)	0.130	0.048	2.35E-02	0.967	0.135	4.78E-03	0.999	3.99E-03	0.904
Pb(II)	0.198	0.018	1.14E-02	0.845	0.197	1.36E-01	1.000	1.49E-03	0.852

also the experimental sorption capacity $q_{m(exp)}$ for the pseudo-second-order model. As previously mentioned, the pseudo-second-order model reflects a rate-limiting step. The reasons for the rate-limiting step include external mass transport across the boundary layer surrounding the particle; diffusional mass transfer within the internal structure of the adsorbent particle by a pore, surface, or branched pore; and adsorption at surface sites, such as in chemisorption or physical sorption (22). There are four sequential steps in the adsorption of metals onto porous and granular media: diffusion through a bulk solution, film diffusion, intraparticle diffusion, and adsorption onto a solid surface (26). If intraparticle or pore diffusion is involved in the adsorption of metals, the relationship between the adsorbed amount of metals and square root of time would be linear. However, as shown in Fig. 3(c) and Table 3, the relationship was not linear for As(III), Cd(II), and Pb(II), implying that the pore diffusion process is not a rate-limiting step. These results suggested that the adsorption onto the solid surface is likely to be the main-limiting step in As(III), Cd(II), and Pb(II) sorption processes on NM. For As(V) and Cu(II), there were distinct regions. The first part may be governed by the initial intraparticle transport of metals controlled by the surface diffusion process, and the other part may be controlled by pore diffusion (26).

pH Effect

The pH effect for metal adsorption on NM is shown in Fig. 4. The adsorption amount of Cd(II), Cu(II), and Pb(II) reached plateaus at pH 8.7, 6.3, and 6.0, respectively. The metals adsorbed the basal plane and the edge of NM. The charge of muscovite basal surface is given by the permanent lattice charge which is generated by the element substitution of Al^{3+} for Si^{4+} in the tetrahedral sheets (13). The edge of muscovite consists of silanol (≡Si-OH) and aluminol (≡Al-OH) groups, and can be assigned as ≡S-OH sites. In general, metal cations adsorb onto ≡S-OH sites to form ≡S-O-Me^{+}(19). At low pH, electrostatic repulsion occurs between the positive metal ions and the edge groups of the surface that are positively charged (27). At higher pH, the metal ions precipitate as metal hydroxides. Cu(II) and Pb(II) precipitate above pH 6, while Cd(II) precipitates above pH 8.5 (19).

For both As(III) and As(V), adsorption reached its maximum at pH 5.6 and decreased with further increase or decrease in pH. These results were similar to other research findings (10). Arsenite forms H_3AsO_3, $H_2AsO_3^-$, and $HAsO_3^{2-}$ in order of increasing pH. Arsenate forms H_3AsO_4, $H_2AsO_4^-$, $HAsO_4^{2-}$, and AsO_4^{3-} in order of increasing pH. At pH 5.6, arsenate—which is present as $H_2AsO_4^-$ and $HAsO_4^{2}$—is more strongly adsorbed than arsenite, which is present as H_3AsO_3. The adsorption behaviors of arsenite and arsenate according to pH are similar. Charlet et al. (18) reported that arsenate is reduced to arsenite during adsorption onto the muscovite surface. Therefore, the pH dependence of arsenite and arsenate is similar. However, in this study, the adsorption amount or removal efficiency of arsenate was higher than that of

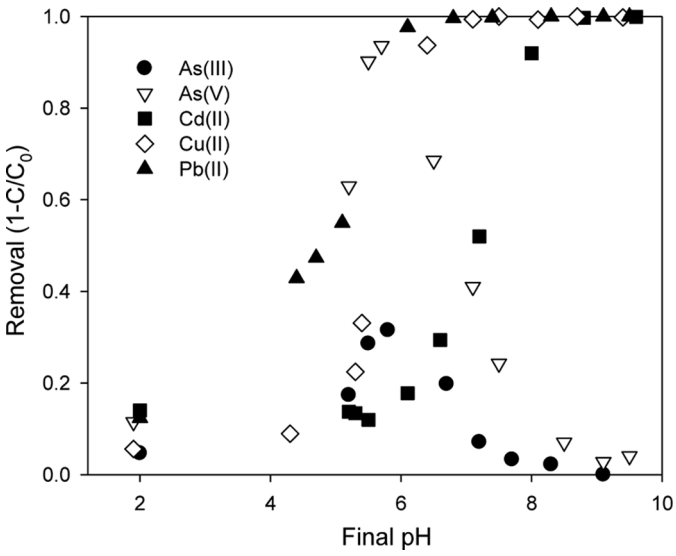

FIG. 4. Effect of pH on the removal of metals by NM.

arsenite. This may have been due to a decrease in or the lack of reduction occurring. A detailed explanation for these results is further discussed in Section titled "The Effect of Ionic Strength."

Adsorption Isotherm

The adsorbed amount of metals onto NM and the equilibrium metal concentrations were fitted using the Langmuir isotherm model (Fig. 5(a)) (28):

$$q_e = \frac{q_{\max} K_L C_e}{1 + K_L C_e}$$

where q_e and q_{max} are the equilibrium and maximum adsorbed amount of metals onto NM ($mg\,g^{-1}$), respectively, K_L is a constant related to the adsorption energy ($L\,mg^{-1}$) and should vary with temperature, and C_e is the equilibrium metal concentration ($mg\,L^{-1}$). This model is based on some assumptions. The metal ions are chemically adsorbed at a fixed number of identical surface sites; each site can capture one metal ion. Sites are energetically equivalent, and there is no interaction between adsorbed metal ions. Therefore, the maximum adsorbed amount of metal ions represents monolayer coverage of metals with muscovite. When fitting with the Langmuir isotherm model, the maximum sorbed amounts of metals q_{max} ($mg\,g^{-1}$) were 0.791, 0.750, 0.630, 0.618, and 0.330 for As(V), Cd(II), Pb(II), Cu(II), and As(III), respectively. The Langmuir parameter K_L ($L\,mg^{-1}$) is related to the adsorption energy of metals onto the solid surface. In experimental results, the order in value was As(V) (0.1723) > Pb(II) (0.0535) > Cu(II) (0.0275) > As(II) (0.0267) > Cd(II) (0.0050). This means that As(V) was strongly sorbed onto NM among the tested metals.

If the adsorbent has multiple adsorption sites, the Freundlich isotherm model is a better choice to describe the experimental data (Fig. 5(b)). The Freundlich isotherm is expressed by (26,29):

$$\ln q_e = \ln K_F + \frac{1}{n} \ln C_e$$

where K_F and $1/n$ are constants. In this study, the Freundlich isotherm model fitted the experimental results better than the Langmuir isotherm model.

The Langmuir and Freundlich isotherm model constants are summarized in Table 4. The regression

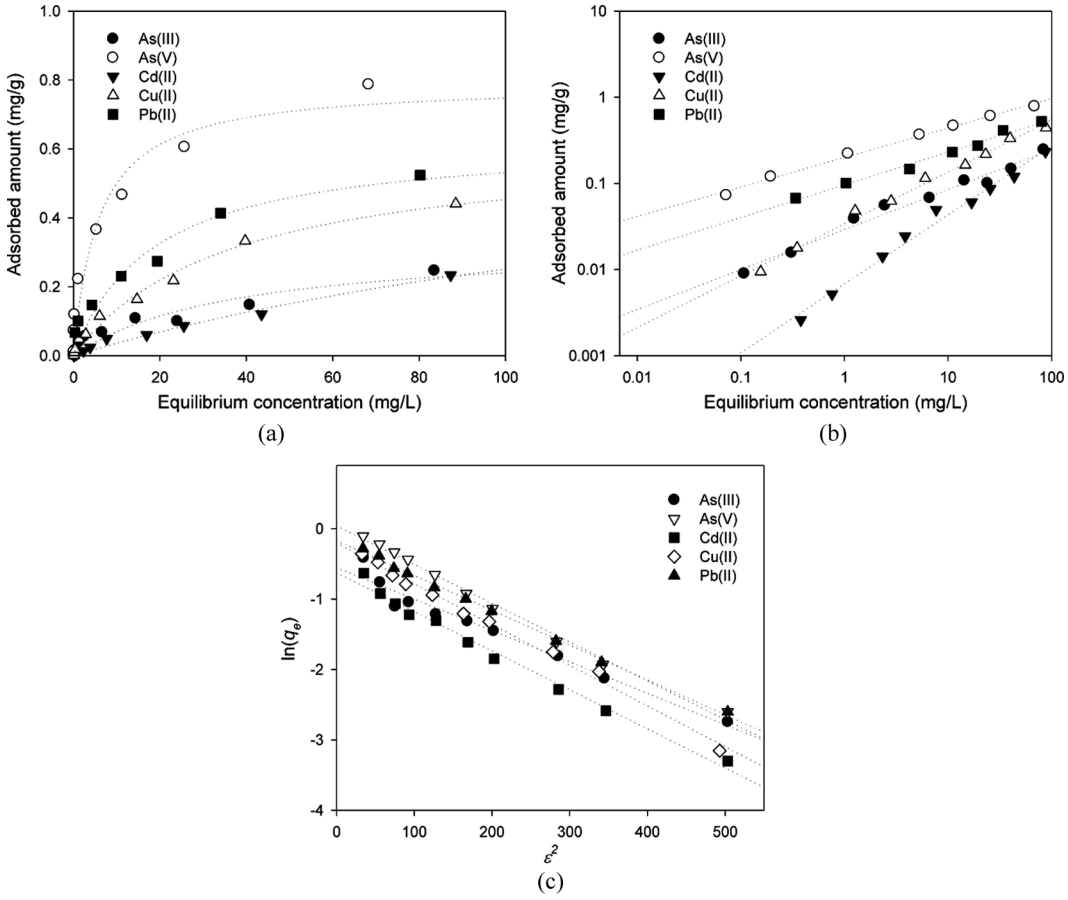

FIG. 5. (a) Langmuir, (b) Freundlich, and (c) DR adsorption model fitting to metal adsorption by NM.

TABLE 4
Adsorption constants for the Langmuir and Freundlich isotherm models

Metal	Langmuir			Freundlich		
	q_{max} (mg g^{-1})	K_L (L mg^{-1})	r^2	K_F (mg g^{-1})(L mg^{-1})$^{1/n}$	$1/n$	r^2
As(III)	0.330	0.0267	0.91	0.029	0.46	0.98
As(V)	0.791	0.1723	0.94	0.200	0.34	0.99
Cd(II)	0.750	0.0050	0.98	0.007	0.80	0.99
Cu(II)	0.618	0.0275	0.99	0.034	0.60	0.99
Pb(II)	0.630	0.0535	0.93	0.096	0.38	0.99

coefficient r^2 with the Freundlich model was 0.98–0.99 and 0.91–0.99 with the Langmuir model. This is because NM is composed of two or more minerals and their surfaces are heterogeneous. The Freundlich isotherm parameter 1/n is the heterogeneity factor. If the $1/n$ value was lower, there is a strong interaction between the metal and adsorbate. The value of $0 < 1/n < 1$ (in this experiment, $0.34 < 1/n < 0.80$) indicates an adsorption slightly suppressed at lower equilibriums and is attributed to the heterogeneous nature of the adsorbents' surface with no interaction between adsorbed ions (30). In this study, NM benefited the adsorption of metals because the $1/n$ values for As(V), Pb(II), As(III), Cu(II), and Cd(II) were 0.345, 0.385, 0.455, 0.588, and 0.769, respectively.

To investigate the adsorption mechanism in more detail, the Dubinin-Radushkevich (DR) equation was applied. The DR equation is based on the heterogeneous surface of the adsorbent and is expressed by (31–33):

$$\ln q_e = \ln q_{\max} - \beta\varepsilon^2$$

where β is the activity coefficient (mol^2 kJ^{-2}) related to the mean sorption energy and ϵ is the Polanyi potential calculated using this equation (34–36):

$$\varepsilon = RT \ln\left(1 + \frac{1}{C_e'}\right)$$

where R is the gas constant (0.00831447 kJ K^{-1} mol^{-1}), T is the absolute temperature (293 K), and C_e' is the equilibrium concentration of metals (g g^{-1}). β is obtained from the slope between $\ln q_e$ and ϵ^2(Fig. 5(c)). The mean free energy E (kJ mol^{-1}) can be calculated from the constant β through the following equation (37).

$$E = 1/\sqrt{2\beta}$$

E provides information on the adsorption mechanism, which is the nature of the interaction between metals and the binding sites (38). If the value is between 8 and 18 kJ mol^{-1}, the adsorption process is chemisorption (chemical adsorption); below 8 kJ mol^{-1}, the adsorption process occurs physically (39,40). The E values for As(III), As(V), Cd(II), Cu(II), and Pb(II) adsorption by NM were 15.6, 14.1, 14.0, 13.9, and 14.9 kJ mol^{-1}, respectively. As a result, it is suggested that the adsorption process occurred chemically. However, according to the recent study on metal adsorption thermodynamics of muscovite (001) surface (15), the adsorption mechanism based on the mean free energy is not always valid. Park et al. (15) reported that the adsorption of Sr^{2+} onto the muscovite (001) surface is driven by electrostatic attraction and the adsorption free energy turns out to be much higher than 8 kJ/mol. These results suggest that the adsorption mechanism should be elucidated by not only free energy but also the studies of interfacial structure.

The adsorption capacity of NM for As(V) was higher than for As(III). Chakraborty et al. (10) reported that As(V) is reduced to As(III) by muscovite and that the adsorption capacity of muscovite for As(III) and As(V) is the same. They mentioned the reason as the reduction from As(V) to As(III) by muscovite. The As3d photoelectron spectra for the NM before and after adsorption with As(III) and As(V) are shown in Fig. 6. The binding energy

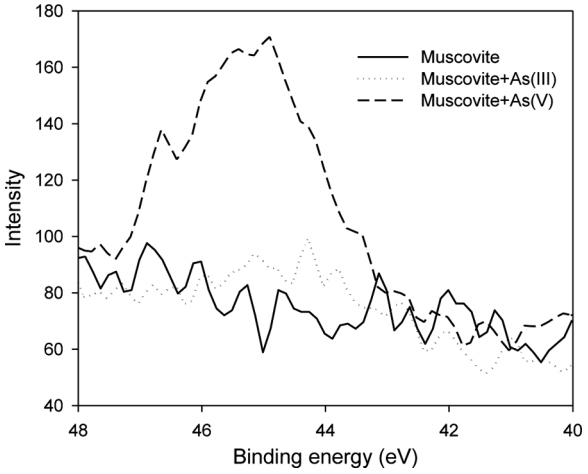

FIG. 6. As3d core level photoelectron spectra of NM with As(III) and As(V).

TABLE 5
Comparison of Langmuir adsorption capacity of NM with those of other mica

	Adsorption capacity ($mg\,g^{-1}$)					
Adsorbent	As(III)	As(V)	Cd(II)	Cu(II)	Pb(II)	Ref.
Muscovite	2.91	2.52				(10)
Biotite	1.05	4.38				(10)
Sericite				1.674	4.697	(19)
Muscovite					20.23	(47)
NM	0.330	0.791	0.750	0.618	0.630	This work

of the As3d core levels of As(III) and As(V) in arsenic oxides are 44.3–44.5 and 45.2–45.6 eV, respectively (18). In Fig. 6, the As3d core level of As(V) spectra shifts slightly toward As(III) when As(V) is adsorbed onto NM. This means that As(V) can be reduced by the muscovite surface (10) but that the reduced amount is relatively small. In addition, the net adsorption amount of metals by NM is lower than that for other purified micas (Table 5). This may be due mainly to impurities in and the surface area of NM. NM contains various minerals such as quartz, muscovite, and undetermined minerals. Because of this composition of NM, the removal mechanism is not the same as that for purified muscovite. These impurities could affect the adsorption process. In addition, the surface area of NM is low. As a result, the amount of As(V) reduced is decreased, and the absolute adsorbed amount of metals is lower.

Effect of Ionic Strength

Figure 7 shows the effect of ionic strength on the adsorption of metals onto NM. The amount of adsorbed metals is slightly affected by ionic strength. In general, the dependence of ionic strength is used to distinguish between specific and non-specific adsorption (19). Farquhar et al. (41,42) used XPS and X-ray absorption fine structure spectroscopy (REFLEXAFS) to study sorption mechanism; they found that Cu(II) and Pb(II) form an inner-sphere complex with a muscovite surface, and Cd(II) forms an outer-sphere complex. Steels et al. (43) used computer simulations and reported that divalent cations such as Cu(II) and Cd(II) do not form strong bonds with the perfect (001) surface of muscovite, where the binding of Cu(II) from solution and the associated loss of $2\,K^+$ ions into the solution are favorable. In this study, the decrease in As(III), As(V), Cu(II), and Pb(II) removal efficiencies was small as ionic strength increased, while Cd(II) removal was relatively suppressed as ionic strength increased (Fig. 7). These results suggested that As(III), As(V), Cu(II), and Pb(II) formed inner-sphere complexes with NM, with Cd(II) forming an outer-sphere complex. But, according to recent studies (15, 44–46), the difference between inner-sphere and outer-sphere complexation was not determined by simple ionic strength experiment. Park et al. (15) reported that the partitioning of Sr^{2+} into a simultaneous inner- and outer-sphere layered structure has been observed. Catalano et al. (45) reported the simultaneous formation of inner- and outer-sphere arsenate surface complexes on hematite and corundum. Consequently, to know the exact adsorption mechanism, a more detailed experiment is required.

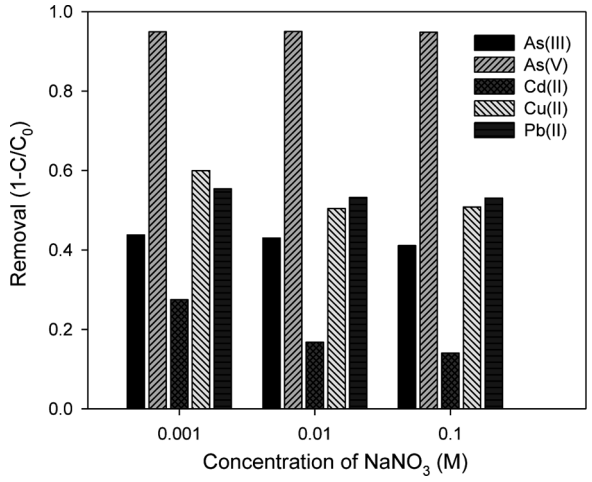

FIG. 7. Effect of ionic strength on the removal of metals by NM.

CONCLUSIONS

NM was applied to the adsorption of metals in aqueous solutions. The elements, Ca, Al, Mg, Fe, K, and Si, were released from NM by dissolution at acidic pH. The adsorption amount of Cd(II), Cu(II), and Pb(II) reached plateaus at pH 8.7, 6.3, and 6.0, respectively. For both As(III) and As(V), adsorption reached its maximum at pH 5.6 and decreased with further increase or decrease in pH. Kinetic studies showed that the pseudosecond-order model explains well the sorption process. With static and kinetic experiment results, it is suggested that the adsorption of metals onto NM is driven by chemisorption and As(III), As(V), Cu(II), and Pb(II) form inner-sphere complexes

with NM whereas Cd(II) forms an outer-sphere complex. But, to elucidate the accurate adsorption mechanism of metals onto natural muscovite, the use of proper spectroscopic technique is required.

In the batch experiments, the maximum adsorption capacities of NM were 0.791, 0.750, 0.630, 0.618, and 0.330 mg g^{-1} for As(V), Cd(II), Pb(II), Cu(II), and As(III), respectively. Although NM is cheaper than purified muscovite, the adsorption capacities of NM are less than those of purified materials. In addition, adsorption is affected by impurities within NM. Therefore, when natural materials are used as adsorptive materials, their purity, composition, and surface characteristics should be seriously considered.

ACKNOWLEDGEMENTS

This research was supported by KIST-Gangneung Institutional program (2Z03290). We thank E.-M. Kim, H.-O. Lee, and Dr. W.-S. Chae at KBSI Gangneung Center for FE-SEM, EDX, and XRD measurements, H.K. Kang at Advanced Analysis Center, KIST for XPS analysis, and M. Hong at FCTIC for XRF and particle size analyses.

REFERENCES

1. Bhattacharyya, K.G.; Sen Gupta, S. (2008) Adsorption of a few heavy metals on natural and modified kaolinite and montmorillonite: A review. *Adv. Colloid Interface Sci.*, 140 (2): 114.
2. Demirbas, A. (2008) Heavy metal adsorption onto agro-based waste materials: A review. *J. Hazard. Mater.*, 157 (2–3): 220.
3. Ngah, W.S.W.; Hanafiah, M. (2008) Removal of heavy metal ions from wastewater by chemically modified plant wastes as adsorbents: A review. *Bioresour. Technol.*, 99 (10): 3935.
4. O'Connell, D.W.; Birkinshaw, C.; O'Dwyer, T.F. (2008) Heavy metal adsorbents prepared from the modification of cellulose: A review. *Bioresour. Technol.*, 99 (15): 6709.
5. Gadd, G.M. (2009) Biosorption: critical review of scientific rationale, environmental importance and significance for pollution treatment. *J. Chem. Technol. Biotechnol.*, 84 (1): 13.
6. Jung, Y.S.; Pyo, M. (2008) Removal of heavy metal ions by electrocoagulation for continuous use of Fe^{2+}/Fe^{3+}-mediated electrochemical oxidation solutions. *Bull. Korean Chem. Soc.*, 29 (5): 974.
7. San Miguel, G.; Lambert, S.D.; Graham, N.J.D. (2006) A practical review of the performance of organic and inorganic adsorbents for the treatment of contaminated waters. *J. Chem. Technol. Biotechnol.*, 81 (10): 1685.
8. Jeon, C.-S.; Baek, K.; Park, J.-K.; Oh, Y.-K.; Lee, S.-D. (2009) Adsorption characteristics of As(V) on iron-coated zeolite. *J. Hazard. Mater.*, 163 (2–3): 804.
9. Kim, M.-S.; Hong, S.C.; Chung, J.G. (2005) Adsorption of Pb(II) on metal oxide particles containing aluminum and titanium in aqueous solutions. *Environ. Eng. Res.*, 10 (2): 45.
10. Chakraborty, S.; Wolthers, M.; Chatterjee, D.; Charlet, L. (2007) Adsorption of arsenite and arsenate onto muscovite and biotite mica. *J. Colloid Interface Sci.*, 309 (2): 392.
11. Gier, S.; Johns, W.D. (2000) Heavy metal-adsorption on micas and clay minerals studied by X-ray photoelectron spectroscopy. *Appl. Clay Sci.*, 16 (5–6): 289.
12. Malani, A.; Ayappa, K.G. (2009) Adsorption isotherms of water on mica: redistribution and film growth. *J. Phys. Chem. B*, 113 (4): 1058.
13. Sposito, G. (1984). *The Surface Chemistry of Soils*, Oxford University Press: New York.
14. Bowers, G.M.; Bish, D.L.; Kirkpatrick, R.J. (2008) Cation exchange at the mineral−water interface: H_3O+/K+competition at the surface of nano-muscovite. *Langmuir*, 24 (18): 10240.
15. Park, C.; Fenter, P.A.; Sturchio, N.C.; Nagy, K.L. (2008) Thermodynamics, interfacial structure, and pH hysteresis of Rb^+ and Sr^{2+} adsorption at the muscovite (001)−solution interface. *Langmuir*, 24 (24): 13993.
16. Bowers, G.M.; Bish, D.L.; Kirkpatrick, R.J. (2008) Cation exchange at the mineral-water interface: H_3O^+/K^+competition at the surface of nano-muscovite. *Langmuir*, 24 (18): 10240.
17. Schlegel, M.L.; Nagy, K.L.; Fenter, P.; Cheng, L.; Sturchio, N.C.; Jacobsen, S.D. (2006) Cation sorption on the muscovite (001) surface in chloride solutions using high-resolution X-ray reflectivity. *Geochim. Cosmochim. Acta*, 70 (14): 3549.
18. Charlet, L.; Chakraborty, S.; Varma, S.; Tournassat, C.; Wolthers, M.; Chatterjee, D.; Ross, G.R. (2005) Adsorption and heterogeneous reduction of arsenic at the phyllosilicate–water interface. In: *Advances in Arsenic Research: Integration of Experimental and Observational Studies and Implications for Mitigation*, O'Day, P.A.; Vlassopoulos, D.; Ming, X.; Benning, L.G., Eds.; ACS Symposium Series Vol. 915, American Chemical Society p. 41.
19. Tiwari, D.; Kim, H.U.; Lee, S.M. (2007) Removal behavior of sericite for Cu(II) and Pb(II) from aqueous solutions: Batch and column studies. *Sep. Purif. Technol.*, 57: 11.
20. Lagergren, S. (1898) About the theory of so-called adsorption of soluble substances. *K. Sven. Vetenskapsakad. Handl.*, 24 (4): 1.
21. Ho, Y.S.; McKay, G. (1998) Sorption of dye from aqueous solution by peat. *Chem. Eng. J.*, 70 (2): 115.
22. Ho, Y.S.; McKay, G. (1998) A comparison of chemisorption kinetic models applied to pollutant removal on various sorbents. *Process Saf. Environ. Protect.*, 76 (4): 332.
23. Ho, Y.S.; McKay, G. (1999) Pseudo-second order model for sorption processes. *Process Biochem.*, 34 (5): 451.
24. Ho, Y.S.; McKay, G. (2000) The kinetics of sorption of divalent metal ions onto sphagnum moss flat. *Water Res.*, 34 (3): 735.
25. Weber, W.J.; Morris, J.C. (1963) Kinetics of adsorption on carbon from solution. *J. Sanit. Eng. Div. ASCE*, 89 (2): 31.
26. Kumar, E.; Bhatnagar, A.; Ji, M.; Jung, W.; Lee, S.-H.; Kim, S.-J.; Lee, G.; Song, H.; Choi, J.-Y.; Yang, J.-S.; Jeon, B.-H. (2009) Defluoridation from aqueous solutions by granular ferric hydroxide (GFH). *Water Res.*, 43 (2): 490.
27. Sari, A.; Tuzen, M.; Citak, D.; Soylak, M. (2007) Adsorption characteristics of Cu(II) and Pb(II) onto expanded perlite from aqueous solution. *J. Hazard. Mater.*, 148 (1–2): 387.
28. Langmuir, I. (1916) The constitution and fundamental properties of solid and liquid. *Part I. Solids. J. Am. Chem. Soc.*, 38 (11): 2221.
29. Freundlich, H.M.F. (1906) Over the adsorption in solution. *Zeitschrift für Physikalische Chemie*, 57 (A): 385.
30. Chutia, P.; Kato, S.; Kojima, T.; Satokawa, S. (2009) Arsenic adsorption from aqueous solution on synthetic zeolites. *J. Hazard. Mater.*, 162 (1): 440.
31. Polanyi, M. (1932) Section III—Theories of the adsorption of gases. A general survey and some additional remarks. Introductory paper to section III. *Trans. Faraday Soc.*, 28: 316.
32. Dubinin, M.M.; Radushkevich, L.V. (1947) Equation of the characteristic curve of activated charcoal. *Proc. Acad. Sci. USSR Phys. Chem. Sect.*, 55: 331.
33. Bering, B.P.; Dubinin, M.M.; Serpinsky, V.V. (1972) On thermodynamics of adsorption in micropores. *J. Colloid Interface Sci.*, 38 (1): 185.
34. Çabuk, A.; Akar, T.; Tunali, S.; Gedikli, S. (2007) Biosorption of Pb(II) by industrial strain of Saccharomyces cerevisiae immobilized

on the biomatrix of cone biomass of Pinus nigra: Equilibrium and mechanism analysis. *Chem. Eng. J.*, 131 (1–3): 293.
35. Fu, L.; Wang, J.; Lu, H.; Su, Y.; Ren, A. (2008) Comment on "The removal of phenolic compounds from aqueous solutions by organophilic bentonite." *J. Hazard. Mater.*, 151 (2–3): 851.
36. Hasany, S.M.; Saeed, M.M. (1992) A kinetic and thermodynamic study of silver sorption onto manganese-dioxide from acid-solutions. *Sep. Sci. Technol.*, 27 (13): 1789.
37. Hobson, J.P. (1969) Physical adsorption isotherms extending from ultrahigh vacuum to vapor pressure. *J. Phys. Chem.*, 73 (8): 2720.
38. Erdem, E.; Karapinar, N.; Donat, R. (2004) The removal of heavy metal cations by natural zeolites. *J. Colloid Interface Sci.*, 280 (2): 309.
39. Helfferich, F.G. (1962) *Ion Exchange*; McGraw-Hill: New York.
40. Rieman, W.; Walton, H.F. (1970) *Ion Exchange in Analytical Chemistry*; 1st; Pergamon Press: Oxford, New York.
41. Farquhar, M.L.; Charnock, J.M.; England, K.E.R.; Vaughan, D.J. (1996) Adsorption of Cu(II) on the (001) plane of mica: A REFLEX-AFS and XPS study. *J. Colloid Interface Sci.*, 177 (2): 561.
42. Farquhar, M.L.; Vaughan, D.J.; Hughes, C.R.; Charnock, J.M.; England, K.E.R. (1997) Experimental studies of the interaction of aqueous metal cations with mineral substrates: Lead, cadmium, and copper with perthitic feldspar, muscovite, and biotite. *Geochim. Cosmochim. Acta*, 61 (15): 3051.
43. Steele, H.M.; Wright, K.; Nygren, M.A.; Hillier, I.H. (2000) Interactions of the (001) surface of muscovite with Cu(II), Zn(II), and Cd(II): A computer simulation study. *Geochim. Cosmochim. Acta*, 64 (2): 257.
44. Fenter, P.; Park, C.; Sturchio, N.C. (2008) Adsorption of Rb^{+} and Sr^{2+} at the orthoclase (001)-solution interface. *Geochim. Cosmochim. Acta*, 72 (7): 1848.
45. Catalano, J.G.; Park, C.; Fenter, P.; Zhang, Z. (2008) Simultaneous inner- and outer-sphere arsenate adsorption on corundum and hematite. *Geochim. Cosmochim. Acta*, 72 (8): 1986.
46. Park, C.; Fenter, P.A.; Nagy, K.L.; Sturchio, N.C. (2006) Hydration and distribution of ions at the mica-water interface. *Phys. Rev. Lett.*, 97 (1): 016101.
47. Pagnanelli, F.; Bornoroni, L.; Moscardini, E.; Toro, L. (2006) Non-electrostatic surface complexation models for protons and lead(II) sorption onto single minerals and their mixture. *Chemosphere*, 63 (7): 1063.